Building and Environment 109 (2016) 112–120

Contents lists available at ScienceDirect

Building and Environment

journal homepage: www.elsevier.com/locate/buildenv

# Experimental study on airflow characteristics of a square column attached ventilation mode

Haiguo Yin*, Angui Li, Zhiyong Liu, Yixiang Sun, Ting Chen

*School of Environmental and Municipal Engineering, Xi'an University of Architecture and Technology, Xi'an, Shaanxi 710055, China*

ARTICLE INFO

*Article history:*
Received 19 July 2016
Received in revised form
1 September 2016
Accepted 7 September 2016
Available online 13 September 2016

*Keywords:*
Ventilation
Air distribution
Square column attached
Experimental
Airflow characteristics

ABSTRACT

A new air distribution pattern, the square column attached ventilation mode, which can be applied to ventilation and air-conditioning systems in large space buildings, is presented in this work. An experimental method was employed to visualize and investigate the airflow characteristics of this novel ventilation mode under isothermal conditions. Our results show the behavior of square column attached ventilation in the form of maximum jet velocity decay, non-dimensional velocity profiles and jet spreading rate at different supply air velocities. The empirical equations governing these characteristic parameters were derived and compared with other types of air jets. The results show that the square column attached ventilation mode is a particular air distribution pattern which combines the advantages of mixing and displacement ventilation. When using the slot outlet with an aspect ratio of 20, the air flow can be treated as a conventional plane wall jet, however the velocity decay and jet diffusion in the occupied zone can be much faster. The obtained results can be helpful in understanding a new air distribution—square column attached ventilation used for ventilation and air-conditioning systems design.


## 1. Introduction

Indoor air distribution determines the diffusion of ventilated air, therefore, affecting indoor air quality and human comfort. Two different ventilation patterns are often used to describe air movement within closed environments, namely Mixing Ventilation (MV) and Displacement Ventilation (DV) [1]. However, MV systems always exhibit a poor ventilation performance [2], and despite their large market share they have low energy efficiency [3]. On the other hand, DV also suffers from some drawbacks such as the large vertical temperature difference, the big air supply inlet, and the inefficiency in the control of floor level contaminants [4,5]. Besides, to avoid the draft sensation, DV systems can only meet moderate cooling loads [6]. To overcome these problems, a series of new ventilation systems have been studied and used.

Karimipanah et al. proposed the Impinging Jet Ventilation (IJV) system based on a vertical wall attached mode [7], which has been widely studied in the following years. Karimipanah et al. focused on evaluating the performance of an IJV system by comparing it with a DV system, and they demonstrated that the IJV system can provide more effective ventilation and more uniform velocity distribution in the occupants' zone [8,9]. Chen et al. discussed a number of important factors influencing the performance of the IJV system [10]. In addition, they also analyzed the impact of the shape of air supply device, supply height, supply airflow rate and supply air temperature on draught discomfort and temperature stratification in an office environment equipped with the IJV system [11]. Yao et al. studied the flow behavior of an isothermal impinging jet in a closed cabin, and improved the performance of the IJV system by using a multi-scale analysis technique based on empirical mode decomposition [12].

Melikov et al. developed the Personalized Ventilation (PV) to control the local building environment [13], and found that PV combined with chilled ceiling can protect occupants from the cross-infection [14]. Yang compared PV, MV and DV, and found PV systems have the potential to maintain a healthier environment at each workstation [15]. With individually controlled micro-environments, PV also has the potential to satisfy more occupants [16]. Makhoul et al. used CFD to analyze the energy saving potential of PV systems, demonstrating that PV reduced energy saving by up to 13% with respect to a conventional MV system [17]. Furthermore, the localized air conditioning system reduced energy consumption by up to 34% using a low-mixing ceiling-mounted PV system [18]. Chen et al. concluded that increasing the ambient temperature is potentially helpful for the decrease of energy consumption in a PV

* Corresponding author. No. 13, Yanta Road, Xi'an, 710055 Shaanxi Province, China.
*E-mail address:* yinhaiguo@xauat.edu.cn (H. Yin).

http://dx.doi.org/10.1016/j.buildenv.2016.09.006
0360-1323/

system, and the best results so far have been obtained with an ambient temperature of 26 °C [19].

Cho et al. studied the formation of Wall Confluent Jets (WCJ) when circular jets, issuing from different apertures in the same plane, flow in parallel directions [20]. Compared to conventional ventilation systems, the effectiveness of ventilation and heat removal was improved in the WCJ mode [21]. In addition to that, Janbakhsh et al. studied the flow behavior of isothermal and non-isothermal WCJ systems in a mock-up office environment, demonstrating that the WCJ device operating at a lower airflow supply rate provides greater thermal comfort for the occupant [22]. Arghand et al. found that WCJ systems have higher air exchange efficiency and are suitable for open-plan offices [23].

Lin et al. provided the Stratum Ventilation (SV) mode, applied in high temperature air-conditioner systems [24]. Their experimental and numerical results demonstrated that the flow pattern formed by stratum ventilation performs well in terms of indoor air quality (IAQ) in the breathing zone [25]. In such conditions, the occupants can have the comfortable feeling of cool head and warm feet, with low draft risk at a room temperature up to 27 °C [26]. With properly designed air supply parameters, SV can be applied in a room with multiple rows of occupants [27].

Furthermore, Li et al. [28,29] and Yin et al. [30] introduced the Air Curtain Ventilation (ACV) system based on the vertical wall attached theory. Cao et al. also investigated an Attached Plane Jet (APJ), however their jet supply device was mounted on the ceiling, in such a way that the jet flow could attach to both the ceiling and the vertical wall [31,32]. These new systems can achieve different goals, including higher ventilation efficiency, larger cooling or heating capacity, better indoor air quality, or human thermal comfort.

In general, the ventilation modes described above are mainly used in offices, hotel rooms or, in general, in situations of small room size and low spatial depth. In large space buildings such as shopping malls and subway stations, these modified ventilation modes are not applicable. In most of these buildings, a large portion of the market is occupied by system based on the stratified air conditioning mode, or on the air supply by using ceiling mounted swirl diffusers. Both of them belong to the traditional MV system, with the inherent disadvantages [33]. However, in order to meet the requirements deriving from the building structure, lots of square columns with smooth surfaces are usually distributed uniformly in large buildings. If ventilation systems were combined with this kind of columns, it may be possible to avoid the influence of building structure and room size. Therefore, based on the advantages of the existing ventilation modes, the square column attached ventilation (SCAV) mode is presented [34,35].

## 2. Principle of SCAV

The estimated airflow pattern of the SCAV mode is shown in Fig. 1a, which is based on the plane wall jet and impinging jet systems [36]. In order to reveal the airflow mechanism of this novel mode, a preliminary visual experimental verification was made under three supply air velocities, as shown in Fig. 1b. According to the value recommended by ASHRAE 55 [37] for the indoor airflow design, the air velocity values of 1.0, 1.5 and 2.0 m/s were used. The supply air velocity was tested according to the method of ASHRAE 70 [38].

As shown in Fig. 1a, the processed air is first delivered from the ambulatory shaped slot, and then it attaches to the column surface and moves downward due to the Coanda effect [39,40]. As the air jet with high momentum approaches the floor, it impinges the column-floor corner, and then separates from the column surface and reattaches to the floor. SCAV can be regarded as a mixing ventilation just before the supply air enters into the occupied zone, where it spreads over the floor causing the jet momentum to recede while still having sufficient force to reach long distances. Furthermore, the air expands in a radial pattern and behaves as a stratified flow, which is similar to the displacement ventilation to some extent. Therefore, the SCAV mode combines some of the characteristics of mixing and displacement ventilation.

These considerations were validated by experimental visualization. As shown in Fig. 1b, the supply air can be attached to the square column, which leads to a lower degree of mixing with the ambient air. The upper fresh air with high capacity can subsequently be brought into the lower occupied zone in the most effective manner, thus contributing to a high ventilation efficiency and a better IAQ. In addition, with the increase of supply air velocity, the main body thickness of attached supply air becomes thinner, which corresponds to a lower degree of mixing between supply air and ambient air, and this is helpful to promote ventilation efficiency. In the occupied zone, the resulting flow by SCAV

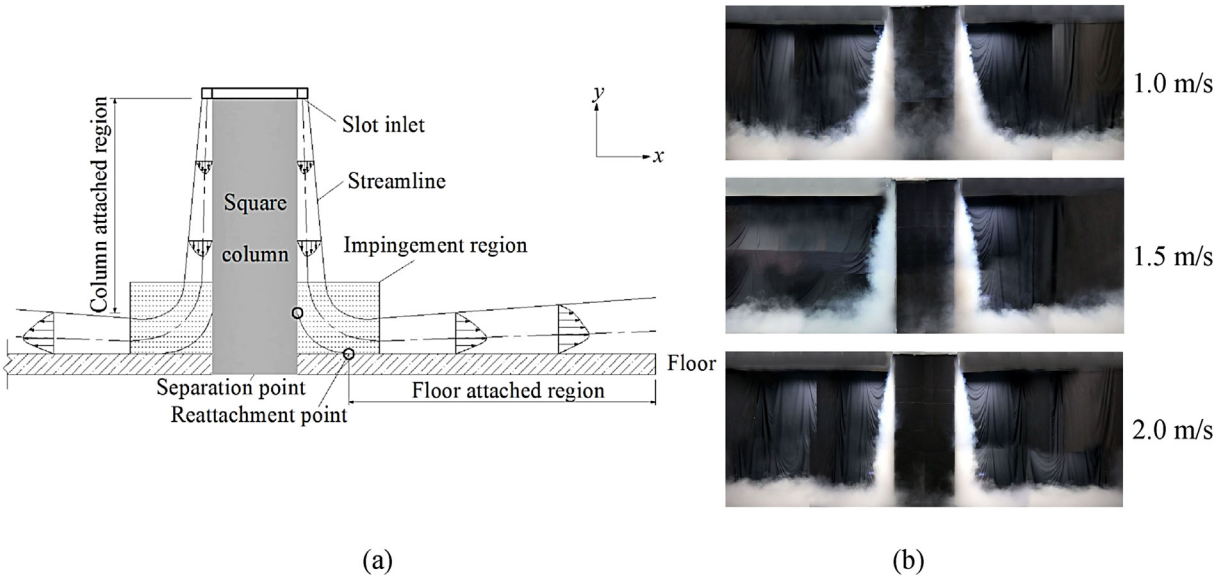


**Fig. 1.** (a) Airflow schematic of square column attached ventilation and (b) visualization experimental verification under different supply air velocities.

causes the so-called “air lake” or “air pool” phenomenon, which characterized as a very thin layer of air over the floor. Similarly to a the DV system, in these conditions a comfortable environment can be created for the occupants. However, unlike the DV system, the air diffusers of the SCAV mode are located on the upper space of the room, which makes them easy to install, and beautiful to display, while it avoids taking up the space of the occupied zone. Thus, the SCAV mode combines the benefits of the ceiling mixing and the wall displacement ventilation systems, demonstrating promising applications.

The aim of this study is to introduce a new attached ventilation mode, performing a detailed investigation on its flow field properties. An air distribution experiment was developed to measure the typical parameters of airflow characteristics, such as the maximum jet velocity decay, the non-dimensional velocity profile and the rate of spread along the attached surface. The test results also compared with the data available from the literature. The current study can open the way to further research on the SCAV mode, helping to improve the air distribution in buildings.

## 3. Experiment

### 3.1. Properties of SCAV

To some extent, the airflow characteristics of SCAV are similar to those of wall jet in the vertical column attached zone and in the horizontal floor attached zone, and air behaves as an impinging jet in the column-floor corner [41]. Therefore, the airflow field can be divided into three regions, as shown in Fig. 1a: (i) the column attached region, (ii) the impingement region and (iii) the floor attached region. However, earlier studies have revealed that the air distribution in the impingement region can be merged with the other two attached regions [42]. Meanwhile, as the square column has four surfaces, a junction flow appears when the supply air from two adjacent surfaces enters the occupied zone. The floor attached region should thus be further divided into a primary floor attached region and a confluent floor attached region. In general, the airflow characteristic study of SCAV will be developed in three regions: (I) the column attached region, (II) the primary floor attached region and (III) the confluent floor attached region.

### 3.2. Test chamber and facilities

The experiment was carried out in a chamber with size of 6.6 m × 6.6 m × 3.15 m ($L \times W \times H$), as shown in Fig. 2a. A fabric curtain covers on the chamber wall, in order to provide a black background to visualize the white smoke in the visualization experimental. The existed fabric curtain didn't have influence on the airflow patterns. Conversely, in the velocity field measurements process, the fabric curtain is removed. The square column, with a size of 1.0 m × 1.0 m × 2.5 m ($l \times w \times h$) is located at the center of the room. There is an air supply device (2.5 m × 0.5 m × 0.5 m) on the top of column, which is built to improve the outlets uniformity by introducing partition plane and perforated plane. These planes can convert the dynamic pressure of the supply air to static pressure. Four linear slot outlets are located at the bottom of this device, with an aspect ratio of 20, corresponding to a length $l$ of 1.0 m and a width $b$ of 0.05 m. The vertical distance between the slot outlets and the floor is 2.5 m (ceiling height). In this experiment, the air from the slot was supplied by a centrifugal fan with an air volume of 2000 $m^3$/h, and the supply air velocity was regulated by a throttle valve, as shown in Fig. 2b.

Before the velocity field measurements, the uniformity among the four slot outlets was tested. The results show that with the help of the rectified device, the outlet velocities from the four slots are similar to each other, with a deviation ranging from 1.8% to 7.3%.Under three supply air velocities of 1.0, 1.5 and 2.0 m/s, the non-uniform coefficients of air speed along the slot length direction are 7.26%, 7.38% and 7.72%, respectively. Therefore, the air supply device can meet the uniformity requirement of the slot outlet air supplying, allowing to focus on a single slot outlet for the next parts of this research.

The distribution of the measurement points is shown in Fig. 3a. According to the properties of SCAV, the velocity field tests were carried out throughout three regions. In order to investigate the three-dimensional characteristics of the SCAV mode, the measured points in each region were distributed along three directions. Fig. 3b represents the measuring point layout of the column attached zone (Region I). The measurement points were set with a non-uniform interval in the airflow direction ($y$-axis), and with a uniform interval of 0.1 m and 0.04 m in the transverse ($z$-axis) and radial direction ($x$-axis), respectively. For the floor attached zone (Regions II and III), the measuring point layout schemes are shown in Fig. 3c and d.

### 3.3. Measurement conditions

As discussed above, the main purpose of this work is to

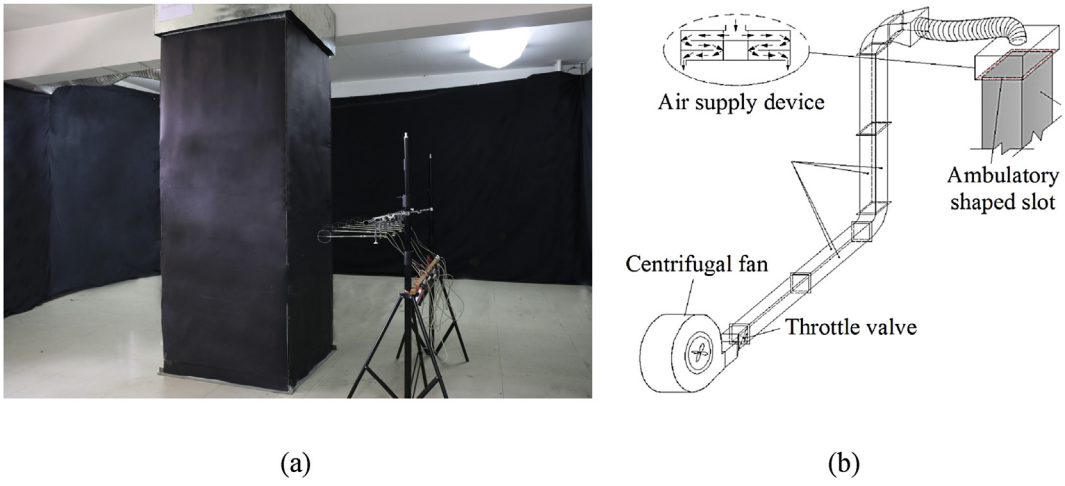


**Fig. 2.** (a) Layout of the SCAV test room and (b) air supply system.

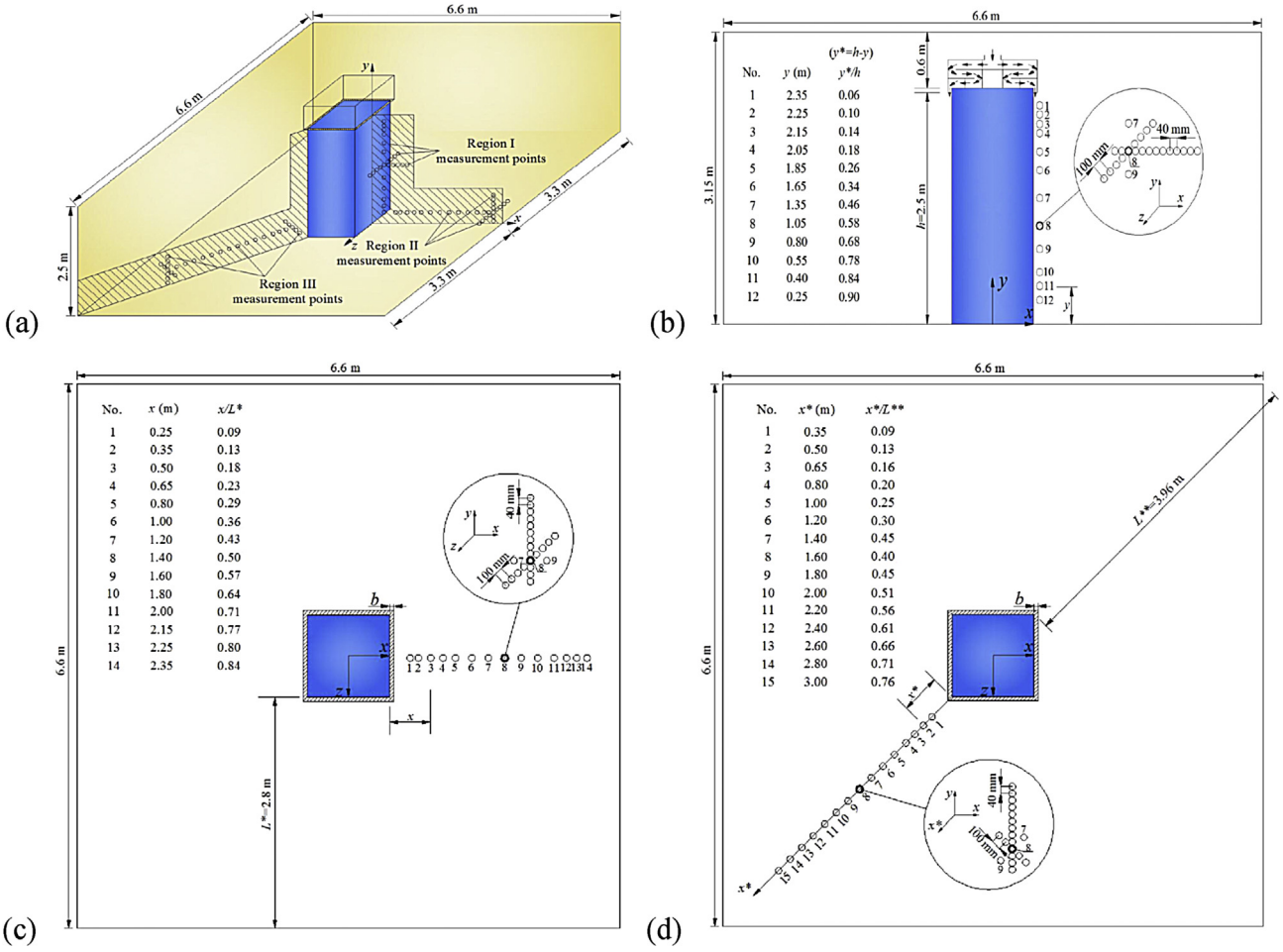


**Fig. 3.** Schematic view of experimental measurement points distribution (a) overview, (b) region I, (c) region II and (d) region III.

**Table 1**
Experimental conditions for isothermal airflow.

| Case | Average slot velocity (m/s) | Supply airflow volume ($m^3$/s) | Ventilation rate (times/h) | Supply air temperature (°C) | Room air temperature (°C) | Reynolds number (slot) |
|---|---|---|---|---|---|---|
| 1 | 1.0 | 0.21 | 7 | 23.7 ± 0.3 | 23.7 ± 0.3 | 3333 |
| 2 | 1.5 | 0.32 | 11 | 24.5 ± 0.3 | 24.5 ± 0.3 | 5000 |
| 3 | 2.0 | 0.42 | 14 | 24.0 ± 0.3 | 24.0 ± 0.3 | 6666 |

introduce the SCAV mode, in order to obtain some airflow characteristics for engineering design, where the isothermal condition is also useful. When used in non-isothermal condition, some correction factors can be introduced by further study. At present, all the cases were measured in undisturbed isothermal conditions, as shown in Table 1.

In order to obtain the accurate time-averaged results for the turbulent airflow, the acquiring period for each measured point was 180 s [43]. Besides, every experimental case was measured three times. When the measured data was similar to each other, the arithmetic mean of these values was used for analysis and presentation.

### 3.4. Measuring instrument and accuracy

Air velocity was measured using a multi-point sampler system manufactured by the SWEMA company from Sweden. This system is equipped with omni-directional draught probes of type SWA 03, which can simultaneously measure the velocity and the temperature. For the velocity, the test range is 0.05–3.00 m/s with an accuracy of ±0.02 m/s at 0.07–0.50 m/s and ±0.03 m/s at 0.50–3.00 m/s. For the temperature, the test range is 10–40 °C m/s with an accuracy of ±0.1 °C. The pressure was measured in the supply duct using a probe of type SWA 10. The test range of this probe is −300–1500 Pa with an accuracy of ±1% read value and minimum of 0.3 Pa. All the probes were calibrated by the manufacturer before the measurements to ensure their accuracy. The results showed that in the testing range of 0.05–2.0 m/s presented in this experiment, the maximum deviation of SWA 03 was 0.012 m/s, which can meet the accuracy requirements.

## 4. Results and discussion

### 4.1. Maximum jet velocity decay

Fig. 4 shows the decay of maximum velocity of the SCAV mode under different supply air velocities in region I, compared with empirical equations for other types of air jets with a slot outlet,

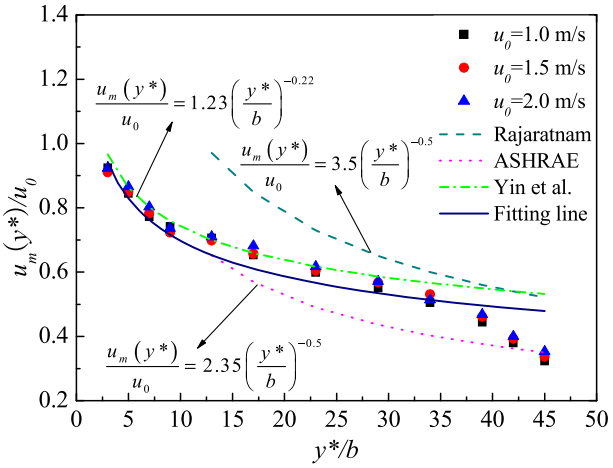


**Fig. 4.** Non-dimensional maximum velocity decay in region I and comparison with other jets.

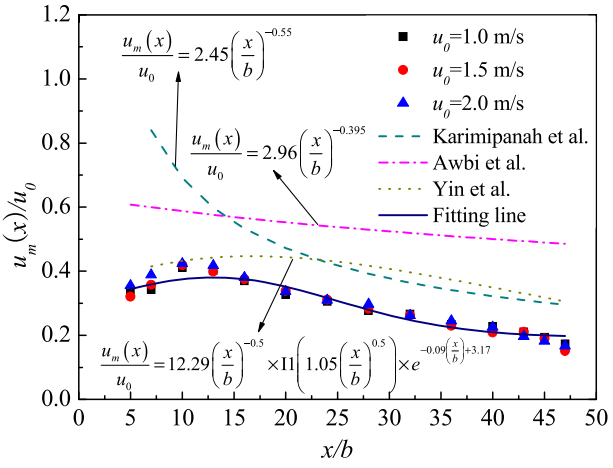


**Fig. 5.** Non-dimensional maximum velocity decay in region II and comparison with other jets.

such as the horizontal plane wall jet developed by Rajaratnam [44] and ASHRAE [45], and the vertical wall attached plane jet introduced by Yin et al. [30].

As shown in Fig. 4, the maximum velocity decay is similar for different slot velocities in region I, while the magnitude of the maximum velocity is proportional to the distance from the slot. Thus, the maximum velocity decay for SCAV can be expressed as:

$$\frac{u_m(y^*)}{u_0}=1.24\left(\frac{y^*}{b}\right)^{-0.25},\ R^2=0.96 \tag{1}$$

where um(y*) is the local maximum velocity at a distance of y* from the slot outlet, u0 is the slot velocity, and b is the width of the slot.

This expression is very similar to the empirical equation used for the vertical wall attached plane jet ($l/b = 2.0/0.05 = 40$). Since the slot aspect ratio of the SCAV mode is 20, the airflow can be treated as a two-dimensional wall jet, thus allowing to neglect the influence of slot length. Meanwhile, the effects of airflow convergence from different column surfaces are limited in region I, and in the whole process of attached airflow, the measured data are approximately in agreement with the values calculated from empirical equation.

For a horizontal plane wall jet, the form of the empirical equations given by Rajaratnam and ASHRAE are similar, differing only by the throw constant. Yu et al. [46] reviewed this aspect in the available literature, finding that the value of the throw constant is located within the range 2.20–3.68 in the developed zone. In the SCAV mode, the developed zone corresponds to the ratio range $13 \le y^*/b \le 39$, and the equation for this zone is given by the expression (2), where the throw constant 2.69 lies in the range derived by Yu. In other words, the airflow characteristics of SCAV can be treated as a traditional plane wall jet in region I, where the influence of jet momentum is more important than that of gravity.

$$\frac{u_m(y*)}{u_0}=2.69\left(\frac{y*}{b}\right)^{-0.5},\ R^2=0.88 \tag{2}$$

Fig. 5 shows the maximum velocity decay of the SCAV mode and other types of air jets in region II. The ventilation patterns used for comparison include, the IJV mode given by Karimipanah et al. [8] that uses a sidewall mounted semicircular or rectangular outlet, the WCJ mode developed by Cho et al. [20] when circular jets issuing from different apertures in the same plane flow in parallel directions, and the ACV mode introduced by Yin et al. [30] that uses a sidewall mounted slot outlet.

As shown in Fig. 5, the maximum jet velocity decay obtained at different slot velocities in region II is also very close to each other. The expression for the decay of maximum velocity in the whole region can be given as:

$$\frac{u_m(x)}{u_0}=0.195+0.186\exp\left[-2\left(\frac{x/b-13}{23.93}\right)^2\right],\ R^2=0.92 \tag{3}$$

where $um(x)$ is the local maximum velocity at a distance of $x$ from the column-floor corner, as shown in Fig. 3c.

This expression is more complicated than expression (1) due to the existence of a speed-up process which occurs at a distance of $5 \le x/b \le 13$. Previous studies have revealed that the air velocity distribution in the corner is nearly symmetric, which means that the maximum jet velocity before the corner is approximately equal to the jet velocity behind it [47]. In region I, the value of maximum jet velocity gradually decreases as the airflow approaches the corner, and a speed-up process subsequently occurs at the beginning stage of region II. Yin et al. also discovered this phenomenon, and predicted the maximum velocity decay by using a Giddings function.

The empirical equations given by Karimipanah and Cho tend to provide inaccurate predictions for the maximum velocity decay at a distance of $5 \le x/b \le 13$, since they are mainly used in the developed zone, and thus cannot account for the speed-up process. For the SCAV mode, the developed zone is approximately found in the range $15 \le x/b \le 45$, and the equation for this zone can be expressed as:

$$\frac{u_m(x)}{u_0}=1.69\left(\frac{x}{b}\right)^{-0.55},\ R^2=0.96 \tag{4}$$

On the other hand, the air diffuser type also has a strong influence on the maximum jet velocity decay. By comparison with that in Fig. 5, we can conclude that the jet momentum by using an aperture confluent outlet is closer to being conserved than in the case of other air diffuser types, such as semicircular outlet, rectangular outlet and slot outlet. In addition, in region II, the SCAV mode using four slot outlets has a larger spreading rate than the ACV mode using a linear slot outlet, which however is helpful for avoiding the draft sensation in the occupied zone. Furthermore, in region I, the maximum velocity decay of the SCAV and the ACV

modes is similar, which means that the fresh air brought into the occupied zone, as well as its capacity, is virtually the same in the two modes. Thus, the square column attached ventilation system produces a better ventilation effectiveness than the air curtain ventilation mode.

Fig. 6 displays the comparison between the maximum jet velocity decays in regions II and III. The velocity distribution is similar in the two regions, with the presence of a speed-up process in confluent floor attached region as well, and the decay of maximum velocity in this region can be given by expression (5), while in the developed zone it can be described by expression (6).

$$\frac{u_m(x^*)}{u_0} = 0.102 + 0.287\exp\left[-2\left(\frac{x^*/b - 10}{42.49}\right)^2\right],\ R^2 = 0.98 \tag{5}$$

$$\frac{u_m(x^*)}{u_0} = 3.84\left(\frac{x^*}{b}\right)^{-0.8},\ R^2 = 0.94 \tag{6}$$

where $um(x^*)$ is the local maximum velocity at a distance of $x^*$, and $x^*$ is the horizontal distance from the column-floor corner, extending along the room diagonal direction, see Fig. 3d.

By contrast, at a distance of $5 \le x^*/b \le 40$, the magnitude of the maximum velocity in region III is larger than that in region II, due to a jet convergence phenomenon. The supply airflow from two adjacent column surfaces converges on the jet boundary with an angle of 45°, and the maximum velocity in region III increases with the mixing of different supply airflows. At a distance of $x^*/b > 40$, a significant proportion of supply air spreads over the floor, which causes the amount of gathering airflow to reduce rapidly. As a consequence, the maximum velocity decay for region III is faster than that for region II, which however is beneficial for avoiding human draught, indicating that this zone may be a good candidate to host resting seats.

### 4.2. Non-dimensional velocity profiles

A plane wall jet is generally defined as issuing from a slot of very large aspect ratio (i.e. $l/b \ge 20$), where any lateral change in the flow properties occurs in a plane normal to the slot length only [48]. For the SCAV mode, the slot outlet aspect ratio is 20 (1.0/0.05). The measured velocity profiles at different air supply velocities are collected and compared with the equations developed by Verhoff [49], Schwarz and Cosart [50] respectively, as shown in Figs. 7–9. Here, $u(x)$ denotes the local velocity at a distance $x$ from the slot outlet at a different height normal to the column surface, $u(y)$ indicates the local velocity at a distance $y$ from the column-floor corner at a different height normal to the floor, $\eta$ is equal to $x/b_{0.5}$ in region I and $y/b_{0.5}$ in regions II and III, and $b_{0.5}$ is the value of $x$ or $y$ at which the velocity $u$ is half its maximum velocity $u_m$.

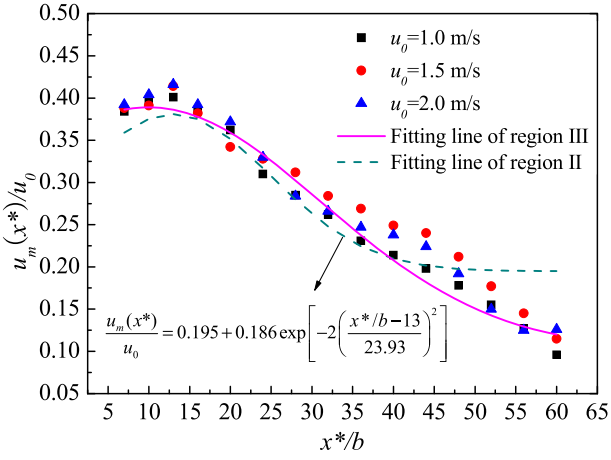


**Fig. 6.** Comparison of non-dimensional maximum velocity decay between regions II and III.

Fig. 7 presents the velocity profiles distribution in region I at different vertical distances from the floor. The dimensionless velocity profiles in the fully developed region are the same as those of a plane jet. The measured velocity profiles are similar to each other and exhibit a Gaussian error curve. In addition, with increasing supply air velocity, the jet velocity profiles become increasingly self-similar. The column surface can 'protect' the supply airflow and reduce the entraining of ambient air, so that a higher ventilation efficiency can be obtained.

The empirical equations of Verhoff and Schwarz for a horizontal plane wall jet are also plotted on Fig. 7 for comparison. The measured velocity profiles present good correlation with the two equations. However, the most significant agreement is found between the experimental data and Verhoff equation, which can be used for predicting the velocity profile of the SCAV mode in region I.

The same procedure is repeated for the floor attached zone as shown in Figs. 8 and 9, which display the empirical equations and the experimental velocity profile results of region II and III, respectively.

As shown in Figs. 8 and 9, for the floor attached zone, a similar non-dimensional velocity profile also appears at different distances from the impinging corner. However, the self similarity of the different velocity profiles in the floor region is not as good as in the vertical region. Under a lower supply air velocity of 1.0 m/s, the dissimilarity characteristics are mainly due to the low momentum, as the supply air does not have sufficient force to spread over the floor and reach a long distance. For a higher velocity of 2.0 m/s, the different similarity characteristics are caused by a stronger impinging on the column-floor corner. In general, the self-similarity of the jet velocity profiles can be enhanced by a higher supply air velocity. The equation given by Verhoff is more accurate than Schwarz's equation in this case as well, and it can be used for predicting the velocity profile of the SCAV mode in the floor attached zone of regions II and III.

### 4.3. Jet spread rate

In order to calculate the jet spread rate, we considered the line representing $b_{0.5}$, to characterize the thickness of the wall jet. Fig. 10 shows the measured values of $b_{0.5}$ at different distances from the slot supply opening in region I, and compared with data obtained from empirical models available in the literature. These models include the horizontal plane wall jet developed by Rajaratnam [44], the impinging jet provided by Beltaos and Rajaratnam [41], and the vertical wall attached plane jet introduced by Yin [42]. The same procedure is repeated for the other two regions, and the corresponding results are presented in Figs. 11 and 12.

As shown in Fig. 10, the supply air velocity has little influence on the jet spread rate, the measured values $b_{0.5}$ being nearly the same at different distances. We performed a best line fit through the measured values under different supply air velocities in region I, obtaining the following relation

$$b_{0.5} = 0.091(y^* + 0.75),\ R^2 = 0.99 \tag{7}$$

The spreading rate of SCAV mode is 0.091, which is very close to the spread rate obtained by Beltaos and Yin, who considered the airflow direction to be the same as that of gravity. By contrast, in the

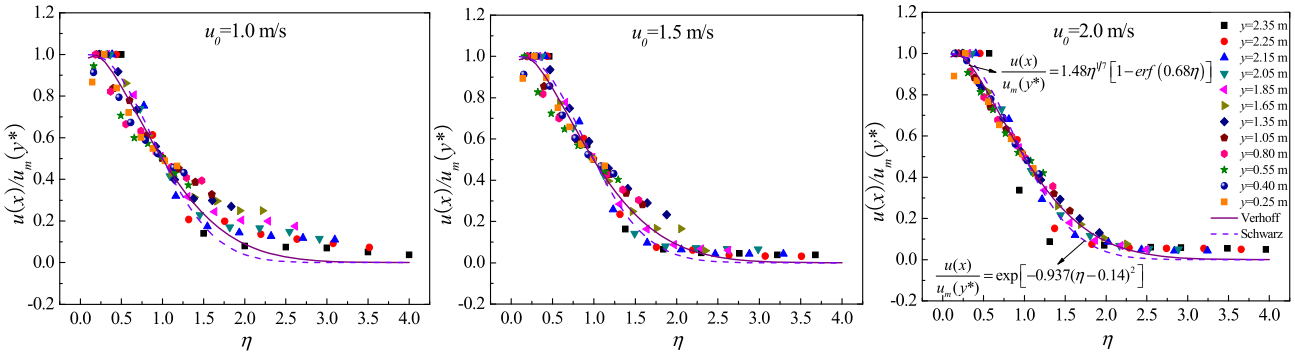


**Fig. 7.** Non-dimensional velocity profiles distribution in region I.

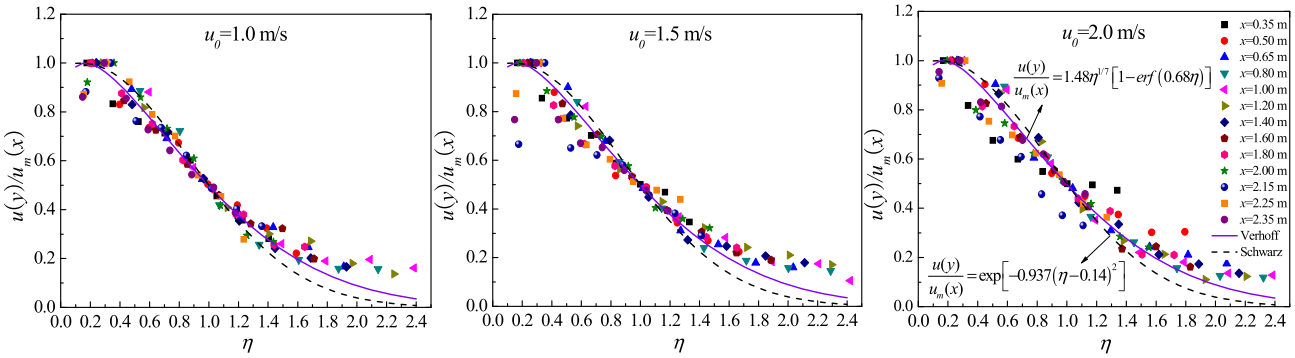


**Fig. 8.** Non-dimensional velocity profiles distribution in region II.

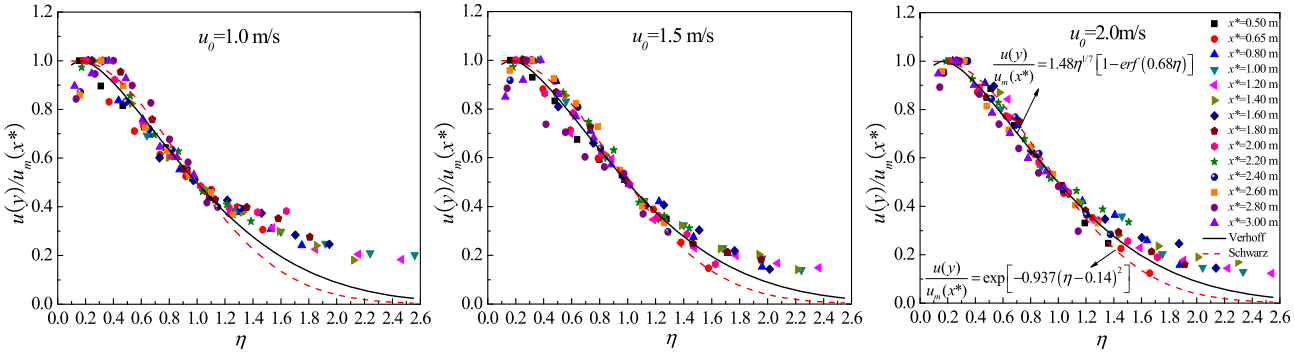


**Fig. 9.** Non-dimensional velocity profiles distribution in region III.

horizontal plane wall jet developed by Rajaratnam, gravity is always perpendicular to the direction of airflow motion. This is helpful to reduce jet diffusion, leading to a lower value of 0.068 for the spreading rate. In addition, the vertical wall attached plane jet is also based on the principle of the impinging jet, which means that the airflow characteristics of the SCAV mode can be studied as a half of a traditional impinging jet.

As shown in Fig. 11, due to the existence of a speed-up process in the floor attached zone, at first there is a jet shrinkage at a distance of $7 \le x/b \le 20$, and then jet diffusion occurs at a distance of $20 \le x/b \le 47$. Thus, the measured values of $b_{0.5}$ decrease at first and then increase, however the measured values under different supply air velocities can also be fitted well with the following expressions.

$$b_{0.5} = -0.18(x - 1.61),\ R^2 = 0.99\ 7 \le x/b \le 20 \quad (8)$$

$$b_{0.5} = 0.101(x + 0.24),\ R^2 = 0.98\ 20 \le x/b \le 47 \quad (9)$$

The same phenomenon was also obtained by Yin, who found a lower spreading rate with respect to the SCAV mode due to the much faster decay of supply airflow by using the SCAV mode in the occupied zone, as displayed in the configuration in Fig. 5. In addition, comparison with the results from Rajaratnam and Beltaos in the developed zone also shows that the jet diffusion of the SCAV mode is the fastest. Meanwhile, compared with the traditional impinging jet, the confinement effect of the column square in the SCAV mode is significant, so that the jet thickness after turning to horizontal direction is smaller than in a free impinging jet. In the current situation, this is more helpful for a uniform diffusion of supply air in the occupied zone.

As shown in Fig. 12, a jet shrinkage phenomenon also occurs in the confluent floor attached region, but the operating distance is

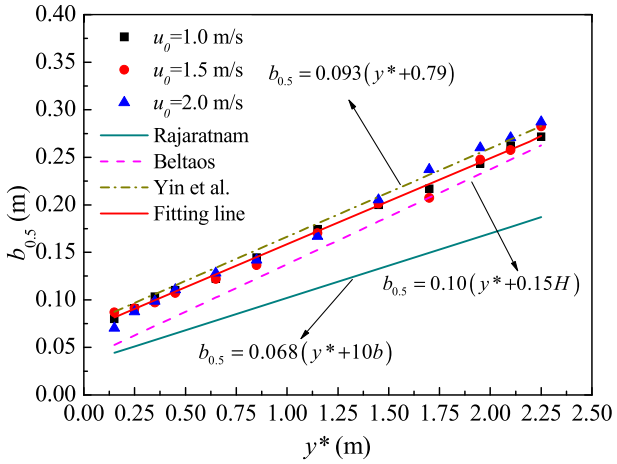


**Fig. 10.** Spreading rate in region I and comparison with other jets.

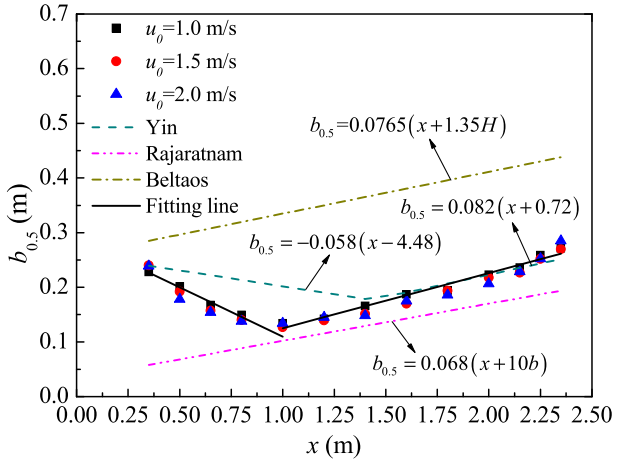


**Fig. 11.** Spreading rate in region II and comparison with other jets.

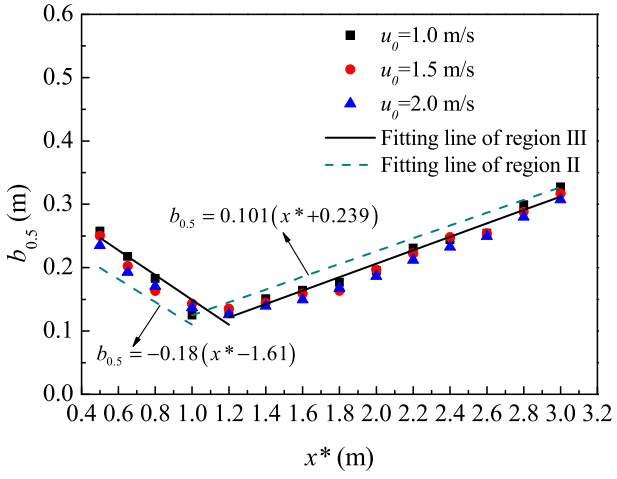


**Fig. 12.** Comparison of spreading rate between regions II and III.

slightly longer than that of region II. The fitting lines also show good agreement with the measured values under different supply air velocities in region III, and the jet spread rate equation for this zone can be expressed as

$$b_{0.5} = -0.196(x^* - 1.76),\ R^2 = 0.9110 \le x^*/b \le 24 \quad (10)$$

$$b_{0.5} = 0.106(x^* - 0.05),\ R^2 = 0.9824 \le x^*/b \le 60 \quad (11)$$

The rate of spread and jet thickness in the two regions are similar to each other, thus, when the supply airflow impinges the column-floor corner and turns into the floor direction, it can spread over the floor at different directions and travel as a plane jet. The resulting flow by SCAV can actually generate the “air lake” or “air pool” phenomenon in the occupied zone, which is promising in terms of applications as discussed in the previous sections.

## 5. Conclusions

The airflow characteristics of square column attached ventilation (SCAV) were investigated experimentally under isothermal conditions. The results show that the flow field of the SCAV mode can be classified into three regions: the column attached region, the primary floor attached region and the confluent floor attached region. The empirical equations for the decay of maximum velocity, the non-dimensional velocity profiles and the rate of jet spread in these regions were obtained and compared with empirical solutions for similar jets taken from the literature. Based on the experimental results and on such comparisons, the following conclusions can be drawn:

The present study shows that the SCAV mode combines the benefits of traditional mixing with those of displacement ventilation systems, and its air distribution can be used for ventilation and air-conditioning systems, especially in the case of large space buildings.

In the column attached region, the comparison of air distribution with other jets shows a similarity between the features of SCAV and of wall jet. The supply air issuing from a slot with an aspect ratio of 20 can be treated as a conventional two-dimensional plane jet.

In the primary floor attached region and in the confluent floor attached region, the airflow travels as a plane jet and its characteristics are similar in both regions. As a result, a uniform distribution of supply air can be created in the occupied zone. After the supply air impinged the column-floor corner, a comparison with other jets shows that the maximum velocity decay and jet diffusion of the SCAV mode can be much faster, which is helpful for avoiding human draught in the occupied zone.

The supply air velocity has little influence on the airflow pattern, but under a higher velocity, more fresh air can enter the occupied zone and spread over a sufficient distance on the floor, which contributes to a better IAQ and a higher ventilation efficiency.

## Acknowledgements

This work was supported by the National Natural Science Foundation of China (No. 51408477); and the Natural Science Foundation of Shaanxi Province (No. 2014JQ7235).

## References

[1] ASHRAE, 2001 ASRAE Handbook: Fundamentals, American Society of Heating, Refrigeration and Air-Conditioning Engineers Inc., Atlanta, GA, 2001.
[2] G.Y. Cao, H.B. Awbi, R.M. Yao, Y.Q. Fan, K. Siren, R. Kosonen, J.S. Zhang, A review of the performance of different ventilation and airflow distribution systems in buildings, Build. Environ. 73 (2014) 171–186.
[3] O. Seppänen, Ventilation strategies for good indoor air quality and energy efficiency, Int. J. Vent. 6 (2008) 297–306.
[4] A. Melikov, G. Pitchurov, K. Naydenov, G. Langkilde, Field study on occupant comfort and the office thermal environment in rooms with displacement ventilation, Indoor Air 15 (2005) 205–214.

[5] X. Shan, J. Zhou, W.C. Chang, E.H. Yang, Comparing mixing and displacement ventilation in tutorial rooms: students' thermal comfort, sick building syndromes, and short-term performance, Build. Environ. 102 (2016) 128–137.
[6] S. Hamilton, K.W. Roth, J. Brodrick, Displacement ventilation, ASHRAE J. 46 (2004) 56–58.
[7] T. Karimipanah, M. Sandberg, H.B. Awbi, A comparative study of different air distribution systems in a classroom, in: Proceedings of the ROOMVENT 2000–Air Distribution in Rooms, Reading, 2000. Berkshire.
[8] T. Karimipanah, H.B. Awbi, Theoretical and experimental investigation of impinging jet ventilation and comparison with wall displacement ventilation, Build. Environ. 37 (2002) 1329–1342.
[9] T. Karimipanah, H.B. Awbi, M. Sandberg, C. Blomqvist, Investigation of air quality, comfort parameters and effectiveness for two floor-level air supply systems in classrooms, Build. Environ. 42 (2007) 647–655.
[10] H.J. Chen, B. Moshfegh, M. Cehlin, Investigation on the flow and thermal behavior of impinging jet ventilation systems in an office with different heat loads, Build. Environ. 59 (2013) 127–144.
[11] H.J. Chen, B. Moshfegh, M. Cehlin, Computational investigation on the factors influencing thermal comfort for impinging jet ventilation, Build. Environ. 66 (2013) 29–41.
[12] S.Y. Yao, Y. Guo, N. Jiang, J.J. Liu, Experimental investigation of the flow behavior of an isothermal impinging jet in a closed cabin, Build. Environ. 84 (2015) 238–250.
[13] A.K. Melikov, C. Radim, M. Milan, Personalized ventilation: evaluation of different air terminal devices, Energy Build. 34 (2002) 829–836.
[14] A. Lipczynska, J. Kaczmarczyk, A.K. Melikov, Thermal environment and air quality in office with personalized ventilation combined with chilled ceiling, Build. Environ. 92 (2015) 603–614.
[15] J. Yang, C. Sekhar, D. Cheong, B. Raphael, Performance evaluation of an integrated personalized ventilation-personalized exhaust system in conjunction with two background ventilation systems, Build. Environ. 78 (2014) 103–110.
[16] H. Zhang, E. Arens, D. Kim, E. Buchberger, F. Bauman, C. Huizenga, Comfort, perceived air quality, and work performance in a low-power task-ambient conditioning system, Build. Environ. 45 (2014) 29–39.
[17] A. Makhoul, K. Ghali, N. Ghaddar, Desk fans for the control of the convection flow around occupants using ceiling mounted personalized ventilation, Build. Environ. 59 (2013) 336–348.
[18] A. Makhoul, K. Ghali, N. Ghaddar, Thermal comfort and energy performance of a low-mixing ceiling-mounted personalized ventilator system, Build. Environ. 60 (2013) 126–136.
[19] Y.X. Chen, B. Raphael, S.C. Sekhar, Experimental and simulated energy performance of a personalized ventilation system with individual airflow control in a hot and humid climate, Build. Environ. 96 (2016) 283–292.
[20] Y.J. Cho, H.B. Awbi, T. Karimipanah, Theoretical and experimental investigation of wall confluent jets ventilation and comparison with wall displacement ventilation, Build. Environ. 43 (2008) 1091–1100.
[21] T. Karimipanah, H.B. Awbi, M. Sandberg, C. Blomqvist, Investigation of air quality, comfort parameters and effectiveness for two floor-level air supply systems in classrooms, Build. Environ. 42 (2007) 647–655.
[22] S. Janbakhsh, B. Moshfegh, Experimental investigation of a ventilation system based on wall confluent jets, Build. Environ. 80 (2014) 18–31.
[23] T. Arghand, T. Karimipanah, H.B. Awbi, M. Cehlin, U. Larsson, E. Linden, An experimental investigation of the flow and comfort parameters for underfloor, confluent jets and mixing ventilation systems in an open-plan office, Build. Environ. 92 (2015) 48–60.
[24] Z. Lin, T.T. Chow, C.F. Tsang, K.F. Fong, L.S. Chan, Stratum ventilation – a potential solution to elevated indoor temperatures, Build. Environ. 44 (2009) 2256–2269.
[25] L. Tian, Z. Lin, Q.W. Wang, Comparison of gaseous contaminant diffusion under stratum ventilation and under displacement ventilation, Build. Environ. 45 (2010) 2035–2046.
[26] Y. Cheng, Z. Lin, A.M.L. Fong, Effects of temperature and supply airflow rate on thermal comfort in a stratum-ventilated room, Build. Environ. 92 (2015) 269–277.
[27] Y. Cheng, Z. Lin, Technical feasibility of a stratum-ventilated room for multiple rows of occupants, Build. Environ. 94 (2015) 580–592.
[28] A.G. Li, H.G. Yin, W.D. Zhang, A novel air distribution method – principles of air curtain ventilation, Int. J. Vent. 10 (2012) 383–390.
[29] A.G. Li, H.G. Yin, G.D. Wang, Experimental investigation of air distribution in the occupied zones of air curtain ventilated enclosure, Int. J. Vent. 11 (2012) 171–182.
[30] H.G. Yin, A.G. Li, Airflow characteristics by air curtain jets in full-scale room, J. Cent. South Univ. T 19 (2012) 675–681.
[31] G.Y. Cao, Modelling the Attached Plane Jet in a Room, PhD Thesis, Helsinki University of Technology, Finland, 2009.
[32] G.Y. Cao, J. Kurnitski, M. Ruponen, O. Seppänen, Experimental investigation and modelling of a buoyant attached plane jet in a room, Appl. Therm. Eng. 29 (2009) 2790–2798.
[33] M.N.A. Saïd, R.A. MacDonald, G.C. Durrant, Measurement of thermal stratification in large single-cell buildings, Energy Build. 24 (1996) 105–115.
[34] A.G. Li, P.F. Tao, Y.J. Zhao, H.G. Yin, A ventilation mode based on square column attached jet, China patent, ZL 201010549211.2, Oct. 10, 2012 [in Chinese].
[35] H.G. Yin, T. Chen, Z.Y. Liu, Y.X. Sun, A.G. Li, Air distribution characteristics of air curtain ventilation mode based on square column attached, Heat. Vent. Air Cond. 46 (2016) 128–134 ([in Chinese]).
[36] H.B. Awbi, Ventilation of Buildings, second ed., 2003. Taylor and Francis, London.
[37] ASHRAE, ANSI/ASHRAE Standard 55-2013: Thermal Environmental Conditions for Human Occupancy, American Society of Heating, Refrigerating, and Air-conditioning Engineers Inc., Atlanta, GA, 2013.
[38] ASHRAE, ANSI/ASHRAE Standard 70-2006: Method of Testing the Performance of Air Outlets and Air Inlets, American Society of Heating, Refrigerating, and Air-conditioning Engineers Inc., Atlanta, GA, 2006.
[39] H. Coanda, Device for deflecting a stream of elastic fluid projected into an elastic fluid, United States patent, 2052869, Sept. 1, 1936.
[40] H. Coanda, Fluid propulsion system, United States Patent, 3337121, Aug. 22, 1967.
[41] S. Beltaos, N. Rajaratnam, Plane turbulent impinging jets, J. Hydraul. Res. 11 (1973) 29–59.
[42] H.G. Yin, Study on Design Procedures of Air Distribution by Air Curtain Ventilation with a Linear Slot Diffuser, PhD Thesis, Xi'an University of Architecture and Technology, Xi'an, 2013.
[43] J. Thorshauge, Air-velocity fluctuations in the occupied zone of ventilated spaces, ASHRAE Trans. 88 (1982) 753–764.
[44] N. Rajaratnam, Turbulent Jets, Elsevier, Amsterdam, 1976.
[45] ASHRAE, 1993 ASHRAE Handbook: Fundamentals, American Society of Heating, Refrigeration and Air-Conditioning Engineers, Inc., Atlanta, GA, 1993.
[46] H. Yu, C.M. Liao, H.M. Liang, Scale model study of airflow performance in a ceiling slot-ventilated enclosure: isothermal condition, Build. Environ. 38 (2003) 1271–1279.
[47] G.Y. Cao, M. Ruponen, J. Kurnitski, Experimental investigation of the velocity distribution of the attached plane jet after impingement with the corner in a high room, Energy Build. 42 (2010) 935–944.
[48] E. Förthmann, Turbulent Jet Expansion, National Advisory Committee for Aeronautics, Technical Memorandum, No. TM-789, National Aeronautics and Space Administration, Washington, D.C, 1934.
[49] A. Verhoff, The Two-dimensional Turbulent Wall Jet without an External Free Stream, Princeton University, Princeton, 1963.
[50] W.H. Schwarz, W.P. Cosart, The two-dimensional turbulent wall jet, J. Fluid Mech. 10 (1961) 481–495.